Progress in Neuro-Psychopharmacology & Biological Psychiatry 56 (2014) 18–26

Contents lists available at ScienceDirect

Progress in Neuro-Psychopharmacology & Biological Psychiatry

journal homepage: www.elsevier.com/locate/pnp

Disrupted structural connectivity network in treatment-naive depression

Zhiliang Long [a,1], Xujun Duan [a,1], Yifeng Wang [a], Feng Liu [a], Ling Zeng [a], Jing-ping Zhao [b,*], Huafu Chen [a,*]

[a] Key Laboratory for NeuroInformation of Ministry of Education, School of Life Science and Technology, University of Electronic Science and Technology of China, Chengdu 610054, PR China
[b] Mental Health Institute, The Second Xiangya Hospital, Central South University, Changsha, Hunan 410011, PR China

ARTICLE INFO

Article history:
Received 25 December 2013
Received in revised form 12 July 2014
Accepted 23 July 2014
Available online 1 August 2014

Keywords:
Depression
Diffusion tensor imaging tractography
Graph theoretical analysis
Small-worldness
Structural connectivity

ABSTRACT

Background: Neuroimaging studies suggest that treatment-naive depression (TD) is characterized by abnormal functional connectivity between specific brain regions. However, the question surrounding the structural basis of functional aberrations in TD patients still remains.
Methods: In the present study, diffusion tensor imaging tractography was employed to construct structural connectivity networks in 22 early adult-onset, first-episode TD patients and 19 healthy controls (HC). Graph theory and network-based statistic (NBS) were then employed to investigate systematically the alteration of whole brain structural topological organization and structural connectivity in TD patients.
Results: Graph theoretical analysis revealed that, compared with HC, TD patients exhibited altered structural topological measures, including decreased shortest path length, normalized clustering coefficient, normalized shortest path length, and small-worldness, as well as increased global and local efficiency. NBS results further revealed that TD patients showed two altered structural sub-networks. One sub-network mainly involved connections between the right orbitofrontal cortex (OFC) and the right insula, putamen, caudate, hippocampus, fusiform gyrus, inferior temporal gyrus and lingual gyrus. The other sub-network mainly included connections between the left OFC and the left gyrus rectus, insula, putamen, caudate, thalamus, pallidum and middle occipital gyrus.
Conclusions: The findings suggest that TD patients exhibit a disruption in the topological organization of structural brain networks. The altered orbitofrontal connectivity may particularly contribute to the manifestation of symptoms in TD patients. The abnormalities may facilitate understanding of the functional disturbances of mood and cognition in the disease.

1. Introduction

Depression is a common psychiatric disease characterized by feelings of sadness, guilt, worthlessness, and hopelessness, followed by a high chance of suicide (Jia et al., 2010; Petersen et al., 2001). The emerging functional magnetic resonance imaging (fMRI) technique has recently deepened the understanding of the pathogenesis of the disorder. For instance, Hooley et al. (2009) reported that participants recovered from depression have increased activation in the amygdala and decreased activation in the dorsolateral prefrontal cortex when they responded to criticism from their mothers. Hypoactivation of prefrontal cortex was also observed in depression when they were shown pictures of sad faces (Lee et al., 2008). However, these studies usually recruited depressive subjects taking antidepressant medication, and the findings might be confounded by medication effects. For example, Lui et al. (2011) found distinct functional deficits in the distributed brain networks between depressed patients who show response to antidepressant treatment and those who exhibit no such response, which indicates different pathogenesis between the two clinical subtypes. Thus, a study of treatment-naive depression (TD) may facilitate understanding of the underlying pathophysiological mechanisms in depression, which could improve early diagnosis and therapy.

A number of neuroimaging studies have revealed that abnormal functional cortico-limbic circuits were associated with the pathophysiology of TD patients. For instance, an fMRI study employing a face-matching task (Frodl et al., 2010) reported a functional connectivity bias of the orbitofrontal cortex (OFC) with precuneus and dorsolateral prefrontal cortex in drug-free patients with depression, representing a neural mechanism of processing bias in the disease. Anand et al. (2009) found decreased cortico-limbic functional connectivity in

Abbreviations: TD, treatment-naive depression; HC, healthy controls; DTI, diffusion tensor imaging; SCN, structural connectivity network; MNI, Montreal Neurological Institute; AAL, automated anatomical labeling; NBS, network-based statistic; PET, positron emission tomography; fMRI, functional magnetic resonance imaging; HRSD, Hamilton Rating Scale for Depression; FACT, Fiber Assignment by Continuous Tracking; ROI, regions of interest; FDR, false discovery rate; OFC, orbitofrontal cortex; DMN, default mode network.

* Corresponding authors.
E-mail addresses: chenhf@uestc.edu.cn (H. Chen), zhaojingpingcsu@163.com (J. Zhao).

[1] Zhiliang Long and Xujun Duan contributed equally to this work.

http://dx.doi.org/10.1016/j.pnpbp.2014.07.007
0278-5846/

unmedicated unipolar depression at rest by using an analysis based on regions of interest (ROI). Altered functional connectivity between the amygdala and prefrontal cortex was observed in TD patients during emotional face processing task (Kong et al., 2013) and also under the resting-state condition (Yue et al., 2013). In addition, resting-state fMRI studies reported that TD patients exhibit altered functional connectivity within the default mode network (DMN) (Guo et al., 2013a; Zhu et al., 2012), and between the DMN and the middle temporal gyrus (Ma et al., 2012), anterior cingulate cortex and thalamus (Guo et al., 2013a). Furthermore, neuroimaging studies revealed increased cerebellar functional connectivity with the temporal poles (Liu et al., 2012) and visual recognition network (Guo et al., 2013b), along with decreased functional connectivity with regions within the DMN (Guo et al., 2013b; Liu et al., 2012) in TD patients. Functional abnormalities of these circuits or networks suggest that TD patients possess a multidimensional and system-level disorder rather than a disease of dysfunction in a single brain region. However, the question surrounding the structural connectivity basis of these functional changes in the disease still remains.

The functional circuit integration has been suggested to be significantly constrained by the large-scale structural pathways interconnecting the human functional brain regions (Hagmann et al., 2008; Honey et al., 2009; van den Heuvel et al., 2008). Therefore, the structural connectivity substrate of distributed functional interactions among brain regions should be studied to gain full understanding of the functional disturbances in TD patients. Diffusion tensor imaging (DTI) tractography, which is capable of reconstructing white matter tracts of the human brain, provides powerful strength for the comprehension of the structural connectivity patterns of brain. To the best of our knowledge, only three studies have investigated the structural connectivity in TD patients by employing DTI tractography. The first study (Korgaonkar et al., 2012) reported that several inter-cortical connections have the most discriminative power for classification between treatment-free depression and healthy controls (HC). This study, however, did not investigate structural connectivity of subcortical areas, for example, the basal ganglia, which has been demonstrated critical in depression (Chantiluke et al., 2012; Marchand, 2010). The second study (Fang et al., 2012) found increased structural connectivity within the cortical-limbic circuit in TD patients. The altered connections were further identified as the most discriminating features. This study, however, did not examine structural abnormalities at the network level. A study of TD patients at network level might provide new insights into the disease. The third study (Korgaonkar et al., in press) demonstrated decreased structural connectivity within the DMN and the network which comprises the frontal cortex, thalamus and caudate regions in a large sample of depression. Results of this study, however, might be affected by antidepressant effects. In brief, these previous structural studies 1) mainly focused on the structural connectivity between cortical and limbic regions, or 2) might have results confounded by medication effects. The question of whether TD patients have deficits of structural connectivity across the whole brain, as well as alterations of structurally topological organization at the network level, still remains.

Graph theory, which is capable of investigating the topological organization of the human brain, has attracted considerable attention in studies of healthy subjects (Achard and Bullmore, 2007; Li et al., 2014; Sporns and Zwi, 2004). This technique conceptualizes the brain as a network consisting of a set of nodes and the edges linking these nodes, and has been increasingly applied to brain diseases such as mild cognitive impairment (Bai et al., 2012), Alzheimer's disease (Lo et al., 2010), post-traumatic stress disorder (Long et al., 2013), and multiple sclerosis (Shu et al., 2011). Two fMRI studies have used graph theory to reveal disruptions of the topological organization of the functional brain network in TD patients, which may contribute to disturbances in mood and cognition in the disease (Jin et al., 2011; J. Zhang et al., 2011). However, the structural topological abnormalities of the brain network in TD patients remain unclear.

The principal aim of the present study was to test whether structurally connectional architecture demonstrates abnormality in TD patients by employing DTI tractography and graph theory. Based on previously reported results, we hypothesized that TD patients might exhibit disruption of the topological organization of the whole-brain structural network, as well as connectivity strength within specific sub-networks.

2. Materials and methods

2.1. Participants

Twenty-two right-handed outpatients with early adult-onset, first-episode TD (10 females; age [mean ± SD]: 28.09 ± 9.91 years; education: 12.23 ± 2.62 years; HRSD score: 25.89 ± 6.26) were recruited from the Mental Health Institute, of the Second Xiangya Hospital, Central South University, China. TD patients were diagnosed using the Structured Clinical Interview according to the DSM-IV criteria (Runeson and Rich, 1994). The severity of depression was quantified by using the 17-item Hamilton Rating Scale for Depression (HRSD) (Hamilton, 1967). Only patients with HRSD score larger than 18 were eligible for the present study. Thus, all patients in our current study are diagnosed to have severe depression. Exclusion criteria included any history of neurological diseases or other physical diseases, as well as comorbidities with other disorders (no evidence of schizoaffective disorder, bipolar disorder or Axis II, personality disorders and mental retardation). Patients younger than 18 years or older than 50 years were also excluded. Additionally, the current illness duration was no more than six months.

Nineteen right-handed HC (9 females; age [mean ± SD]: 24.37 ± 4.18 years; education [mean ± SD]: 13.11 ± 2.47 years) were recruited from the community. The participants were interviewed by the same psychiatrists using the Structured Clinical Interview for DSM-IV, non-patient edition (Runeson and Rich, 1994). None of the participants had a history of serious medical or neuropsychiatric illness or a family history of major psychiatric or neurological illness among first-degree relatives. No significant differences in age, gender, and education were found between TD patients and HC. The clinical and demographic data are shown in Table 1.

The present study was approved by the Ethics Committee of the Second Xiangya Hospital, Central South University. All participants were given information about the procedure, and participated in the research willingly and without coercion. Written informed consents were obtained from all participants.

2.2. Data acquisition

All participants were scanned by using a 1.5T GE scanner (General Electric, Fairfield, Connecticut, USA). The participants were asked to use a prototype quadrature birdcage head coil fitted with foam padding to minimize head movement. The participants were instructed to remain motionless, keep their eyes closed and not think of anything in particular. T1 and DTI images were acquired using the following sequences respectively: 1) T1-weighted volumetric 3D Spoiled Gradient Recall sequence (repetition time/echo time [TR/TE] = 12.1/4.2 ms,

Table 1
Demographic information and disease severity in TD patients and HC.

Demographic data	TD (n = 22)	HC (n = 19)	p value
Gender (male/female)	12/10	10/9	0.902[a]
Age (years)	28.09 ± 9.91	24.37 ± 4.18	0.119[b]
Years of education (years)	12.23 ± 2.62	13.11 ± 2.47	0.278[b]
HRSD score	25.89 ± 6.26	–	
Illness duration (months)	2.95 ± 1.73	–	

TD, treatment-naive depression; HC, healthy control; HRSD, Hamilton Rating Scale for Depression.
[a] The p value was obtained by chi-square test.
[b] The p value was obtained by two-tailed two-sample t-test.

matrix = 512 × 512, slices = 172, flip angle = 15°, field of view [FOV] = 240 × 240 mm^2, slice thickness = 0.9 mm, voxel size = 0.51 × 0.51 × 0.9 mm^3; orientation = sagittal); 2) single shot echo planar imaging sequence (TR/TE = 12,000/105 ms, matrix = 128 × 128, slices = 30, flip angle = 90°, FOV = 240 × 240 mm^2, slice thickness = 4 mm, no gap, voxel size = 0.94 × 0.94 × 4 mm^3, orientation = axial, 13 non-collinear diffusion weighting gradient direction [b = 1000 s/mm^2] and one additional image without diffusion weighting [b = 0 s/mm^2]).

2.3. Network construction

In the present study, a structural connectivity network (SCN) was constructed for each participant. The SCN comprised nodes based on the Automated Anatomical Labeling (AAL) atlas (Tzourio-Mazoyer et al., 2002), and edges characterized by fiber tracts connected these nodes. As suggested by previous studies (Gong et al., 2009; Z. Zhang et al., 2011), the following procedures were conducted to determine the nodes and edges of SCN.

ROIs were defined in the native diffusion space (Gong et al., 2009) to determine the nodes of SCN in each participant. Accordingly, each individual T1-weighted image was first co-registered to the B0 image (without diffusion weighting) in the native diffusion space by using a linear transformation. Co-registered structural images were then mapped to the Montreal Neurological Institute (MNI) T1-template by applying an affine transformation with 12 degrees of freedom, along with a series of non-linear warps. The derived transformation parameters were inverted and used to warp the AAL atlas (Tzourio-Mazoyer et al., 2002) from the MNI space to the native diffusion space with nearest-neighbor interpolation. Preprocessing was carried out by using the Statistical parametric Mapping (SPM8, http://www.fil.ion.ucl.ac.uk/spm). With this procedure, 90 cortical and subcortical regions (45 for each hemisphere) were obtained in the DTI native space. A list of anatomic labels of nodes is presented in Table 2.

The edges of SCN were determined as follows. Diffusion-weighted images of each participant were geometrically corrected for stretches and shears attributed to the eddy current distortions. The corrected images were then co-registered to the B0 image using affine transformations to minimize slight head movements. Diffusion tensor models were estimated by the linear least-squares fitting method at each voxel using the Diffusion Toolkit software (Wang et al., 2007). Whole-brain fiber tracking was performed in the native diffusion space for each participant using the Fiber Assignment by Continuous Tracking (FACT) algorithm embedded in the Diffusion Toolkit. Path tracing continued until the fractional anisotropy was less than 0.2 or the angle between the current and the previous path segment exceeded 45°, as suggested in a previous study (Shu et al., 2011).

In the native diffusion space, ROI i and ROI j were considered to be linked through an edge $e = (i, j)$, in case at least one fiber f was present between them. The weight of each edge, $w(e)$, was calculated as the number of fibers normalized by the sum of surfaces of ROI i and ROI j, that is $w(e) = 2N_{i,j}/(S_i + S_j)$(van den Heuvel and Sporns, 2011). In particular, $N_{i,j}$ is the number of fibers between ROI i and ROI j. S_i and S_j are two-dimension intersects of the individual's white matter with AAL ROI i and ROI j, respectively.

2.4. Whole brain network organization

Before estimating the whole brain topological network organization, the SCN of each participant has to be thresholded to be a binarized matrix with 1 representing the number of fibers larger than a given threshold, and 0 otherwise. In our current study, the threshold range of 1 to 5 was applied to each whole brain SCN with an interval of 1, as a previous study suggested (Bai et al., 2012). Several topological measures were calculated for each whole brain binarized matrix.

Table 2
Six anatomical sub-regions and abbreviated regional labels.

Region name	Abbreviation	
	LH	RH
Medial temporal		
Amygdala	lAMYG	rAMYG
Hippocampus	lHIP	rHIP
Parahippocampal gyrus	lPHIP	rPHIP
Middle temporal gyrus, temporal pole	lMTGp	rMTGp
Superior temporal gyrus, temporal pole	lSTGp	rSTGp
Frontal		
Anterior cingulate gyrus	lACC	rACC
Inferior frontal gyrus, opercular	lIFGoper	rIFGoper
Inferior frontal gyrus, orbital	lIFGorb	rIFGorb
Inferior frontal gyrus, triangular	lIFGtri	rIFGtri
Superior frontal gyrus, medial orbital	lSFGmorb	rSFGmorb
Middle frontal gyrus, orbital	lMFGorb	rMFGorb
Middle frontal gyrus	lMFG	rMFG
Superior frontal gyrus, medial	lSFGmed	rSFGmed
Superior frontal gyrus, orbital	lSFGorb	rSFGorb
Superior frontal gyrus	lSFG	rSFG
Gyrus rectus	lREG	rREG
Occipital		
Calcarine fissure	lCAL	rCAL
Cuneus	lCUN	rCUN
Fusiform gyrus	lFG	rFG
Lingual gyrus	lLING	rLING
Inferior occipital gyrus	lIOG	rIOG
Middle occipital gyrus	lMOG	rMOG
Superior occipital gyrus	lSOG	rSOG
Subcortical		
Caudate nucleus	lCAU	rCAU
Olfactory cortex	lOLF	rOLF
Pallidum	lPAL	rPAL
Putamen	lPUT	rPUT
Thalamus	lTHA	rTHA
Parietal-(pre) motor		
Angular gyrus	lANG	rANG
Median cingulate gyrus	lMCC	rMCC
Posterior cingulate gyrus	lPCC	rPCC
Paracentral lobule	lPCL	rPCL
Inferior parietal gyrus	lIPG	rIPG
Superior parietal gyrus	lSPG	rSPG
Postcentral gyrus	lPoCG	rPoCG
Precentral gyrus	lPreCG	rPreCG
Precuneus	lPCUN	rPCUN
Supplementary motor area	lSMA	rSMA
Supramarginal gyrus	lSMG	rSMG
Rolandic operculum	lROL	rROL
Temporal		
Heschl gyrus	lHES	rHES
Insula	lINS	rINS
Inferior temporal gyrus	lITG	rITG
Middle temporal gyrus	lMTG	rMTG
Superior temporal gyrus	lSTG	rSTG

Seven topological measures describing properties of the whole brain network organization were considered: clustering coefficient (C), local efficiency (E_{local}),shortest path length (L), global efficiency (E_{global}), normalized clustering coefficient (γ), normalized shortest path length (λ), and small-worldness (σ). Briefly, C and E_{local} reflect functional segregation. C quantifies the extent of local interconnectivity or cliquishness in the network (Onnela et al., 2005). E_{local} quantifies the fault tolerance of the network, indicating how well each sub-graph exchanges information (Bullmore and Bassett, 2011). High scores on the two measures correspond to highly segregated neural processing (Achard and Bullmore, 2007; Rubinov and Sporns, 2010). L and E_{global} reflect functional integration. L measures the capability for information transfer between brain regions (Latora and Marchiori, 2001). E_{global} is a measure of the overall capacity for parallel information transfer and integrated processing (Achard and Bullmore, 2007). A lower score on L (or higher E_{global}) indicates a more rapid combination of specialized information from distributed brain regions (Rubinov and Sporns,

2010).γ and λ are normalized relative to C and L of the 100 matched random networks that preserve the number of nodes, edges, and degree distribution of the real network. A network would be considered as a small-world network if a small-worldness (σ), calculated by $\sigma = \frac{\gamma}{\lambda}$, is greater than 1.0 (Sporns and Zwi, 2004; Watts and Strogatz, 1998), with a higher value indicating a more optimized balance between local specialization and global integration (Rubinov and Sporns, 2010). The seven topological measures are commonly used as index to quantify network structures in graph theory mathematically. Detailed information on these seven measures was reported in previous studies (Achard and Bullmore, 2007; Bullmore and Bassett, 2011; Rubinov and Sporns, 2010; Sporns and Zwi, 2004).

Between-group difference in each measure was investigated at each threshold between HC and TD patients. The significance of any difference was tested by using two-sample t-test with $p < 0.05$.

2.5. Alterations in sub-networks

In this section, one sample t-test was employed to extract all edges [i.e., w(e)] that met a significance level with the false discovery rate (FDR) corrections ($p < 0.05$) in HC and TD patients. The identified edges within either the TD patients or HC would then be combined into a connection mask used in the following NBS.

The NBS (Zalesky et al., 2010) was used to identify the significance of any connected sub-networks evident in the set of altered connections found in TD patients. The NBS was implemented in the present study as follows: A primary threshold (here, $t = 2.5$) was initially applied to the t-statistic computed for each edge within the connection mask obtained from one sample t-test, to define a set of suprathreshold edges. Any connected components or sub-networks within the set of suprathreshold edges were determined using MATLAB software (Version 8.0) by executing the "components" function. The size of the components (number of edges) was then obtained. The null distribution of the component size was empirically obtained using non-parametric permutation approach (5000 permutations) to estimate the significance of each connected components. For each permutation, each participant was randomly assigned to one of the two groups with the same size as the origin groups of TD and HC. The same threshold ($t = 2.5$) was then applied to determine the suprathreshold edges within the same connection mask, and the maximum component size was computed. A p-value was assigned to each connected component by computing the proportion of component size exceeding the null distribution values. The connected sub-networks with p-value lower than 0.05 were considered significant. A detailed description is given in the study by Zalesky et al. (2010).

Pearson correlation coefficient was computed in TD patients to assess the significance of any linear associations between clinical variables describing the sample characteristics (i.e., HRSD score, and illness duration) and edges within the altered sub-networks. A correlation with $p < 0.05$ was considered significant.

3. Results

3.1. Altered whole brain network organization

Results revealed that both HC and TD groups demonstrated small-world topology. The two-sample t-test further revealed significantly ($p < 0.05$) altered topological measures in TD patients. In particular, TD patients showed lower L, γ, λ, and σ, but higher E_{global} and E_{local} than HC (Fig. 1).

3.2. Altered sub-networks

One sample t-test suggested that, in both groups, the identified edges were located across the whole brain regions. However, more edges were identified in TD patients than in HC (Fig. 2). With FDR correction, 231 edges survived in HC, whereas 397 edges survived in TD patients. These edges were combined into a connection mask consisting of 397 edges.

The NBS revealed two connected sub-networks that were disrupted in TD patients within the connection masks. The first altered sub-network ($p = 0.0062$, corrected) comprised edges between the right orbital part of superior frontal gyrus and the right orbital part of inferior frontal gyrus, insula, and caudate; between the right orbital part of medial frontal gyrus and the right orbital part of inferior frontal gyrus, insula, hippocampus, and putamen; between the right orbital

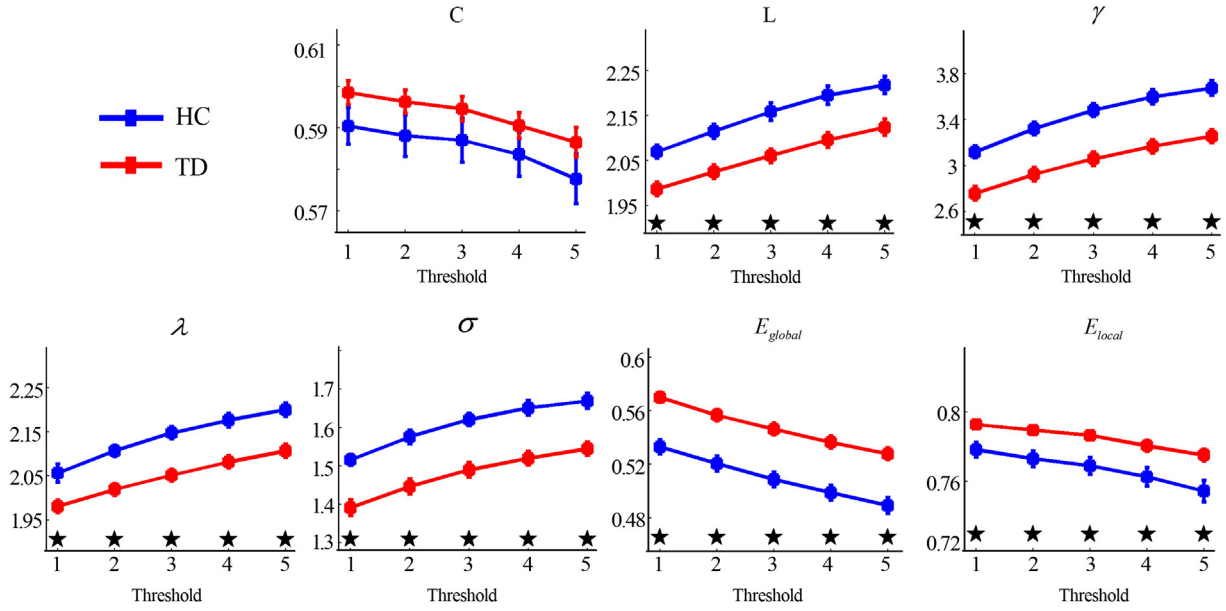

Fig. 1. Topological measures including the C, L, γ, λ, σ, E_{global}, and E_{local} (left to right) of HC (blue lines) and TD patients (red lines) as a function of threshold (number of fibers). The stars indicate the significant difference of the measures between the two groups at each threshold using two-sample t-test. The vertical bar indicates the standard error across subjects in each group. C, clustering coefficient; L, shortest path length; γ, normalized clustering coefficient; λ, normalized shortest path length; σ, small-worldness; E_{global}, global efficiency; E_{local}, local efficiency; HC, healthy control; TD, treatment-naive depression. (For interpretation of the references to color in this figure legend, the reader is referred to the web version of this article.)

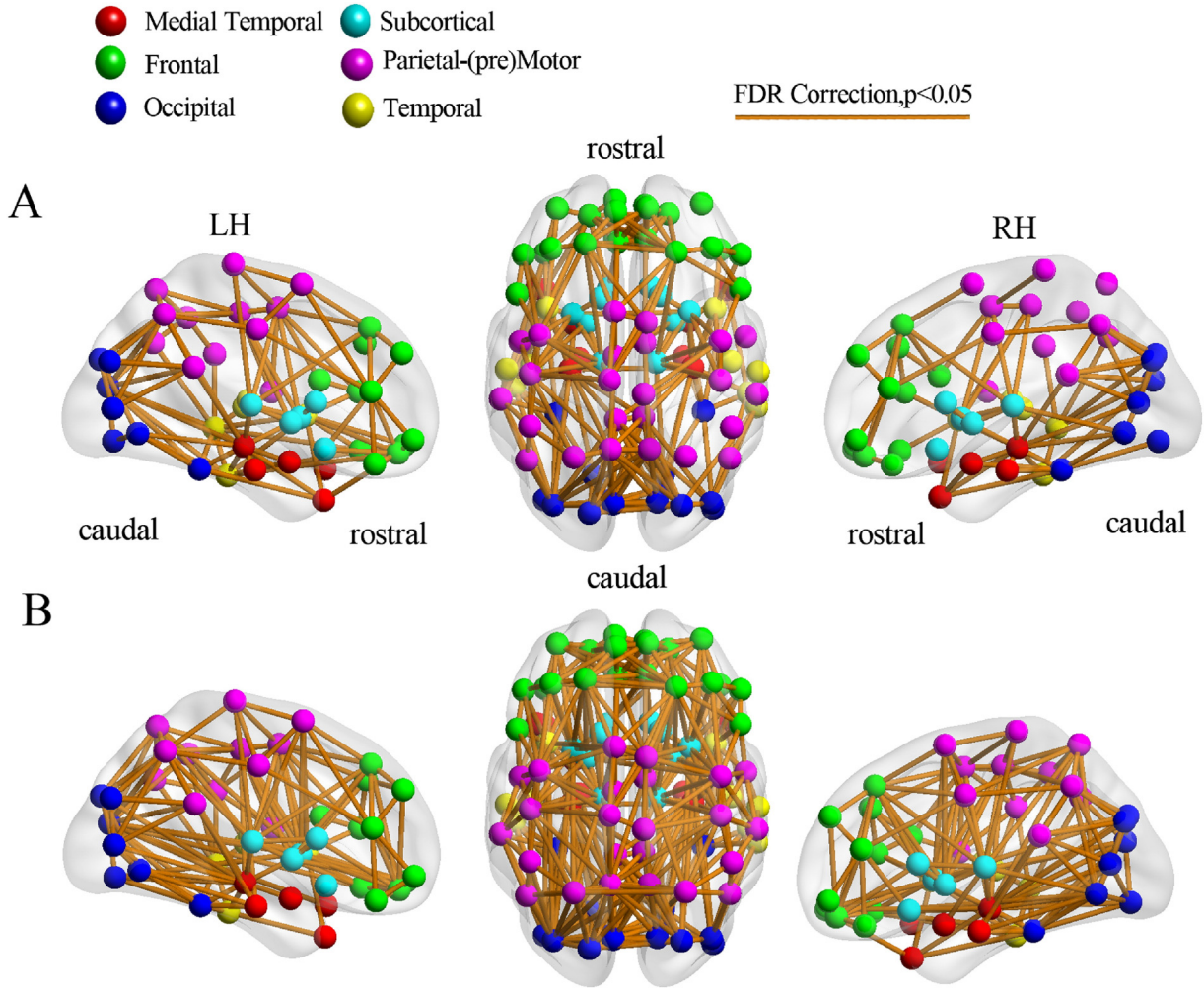

Fig. 2. Visualization of SCN tested by one-sample t-test in HC and TD patients. (A) Dorsal and lateral views of SCN in HC. The six anatomical sub-regions listed in Table 2 are colored differently. The nodes represent brain regions based on AAL atlas, and undirected edges interconnecting pairs of nodes survive the FDR multiple comparison correction with $p < 0.05$. (B) Dorsal and lateral views of SCN in TD patients. SCN, structural connectivity network; HC, healthy control; TD, treatment-naive depression; AAL, anatomical automatic labeling; FDR, false discovery rate. (For interpretation of the references to color in this figure legend, the reader is referred to the web version of this article.)

part of inferior frontal gyrus and the right insula, lingual gyrus, fusiform gyrus, and inferior temporal gyrus; between the right superior frontal gyrus and the right caudate; as well as between the right insula and the right inferior temporal gyrus (Fig. 3A). The second altered sub-network ($p = 0.0054$, corrected) consisted of edges between the left orbital part of superior frontal gyrus and the left orbital part of medial frontal gyrus, rectus, caudate, and putamen; between the left orbital part of medial frontal gyrus and the left insula, putamen, and pallidum; between the left orbital part of inferior frontal gyrus and the left middle occipital gyrus, and pallidum; between the left caudate and the left putamen, pallidum, and thalamus; between the left insula and the left middle occipital gyrus; as well as between the left triangular part of medial frontal gyrus and the left insula (Fig. 3B). Notably, the two sub-networks exhibited increased connections in TD patients compared with HC. The results of the altered sub-network are summarized in Table 3.

No significant correlations were found between clinical variables (including HRSD score and illness duration) and edges within the altered sub-networks.

4. Discussion

The present study provided evidence of altered SCN in TD patients. In particular, the topological organization of SCN was found to be disrupted in TD patients, with decreased values of L, γ, λ, and σ, and increased values of E_{global} and E_{local}. The results indicated a disturbance between local specialization and global integration in TD patients. In addition, TD patients showed increased structural connectivity of OFC with subcortical brain areas, including the putamen, caudate, thalamus, and pallidum, as well as altered connectivity of OFC with several other brain regions, including the insula, hippocampus, inferior temporal gyrus, and fusiform gyrus. These results might provide structural substrates to facilitate understanding of the emotional abnormalities and cognitive bias observed in TD patients.

4.1. Altered whole brain network organization

The first major finding in the present study was the altered whole-brain structural organization of TD patients. The human brain is a complex, interconnected system that has many important topological properties, such as small-worldness, and highly connected network hubs (Bullmore and Bassett, 2011; He and Evans, 2010; Wang et al., 2010). In brain network, small-worldness is an attractive model reflecting two fundamental organizations: functional segregation and functional integration. The former characterizes the ability for specialized processing to occur within densely interconnected groups of brain regions, whereas the latter characterizes the ability for information communication between distributed brain regions. In the present study, both HC and TD patients showed small-world topology in

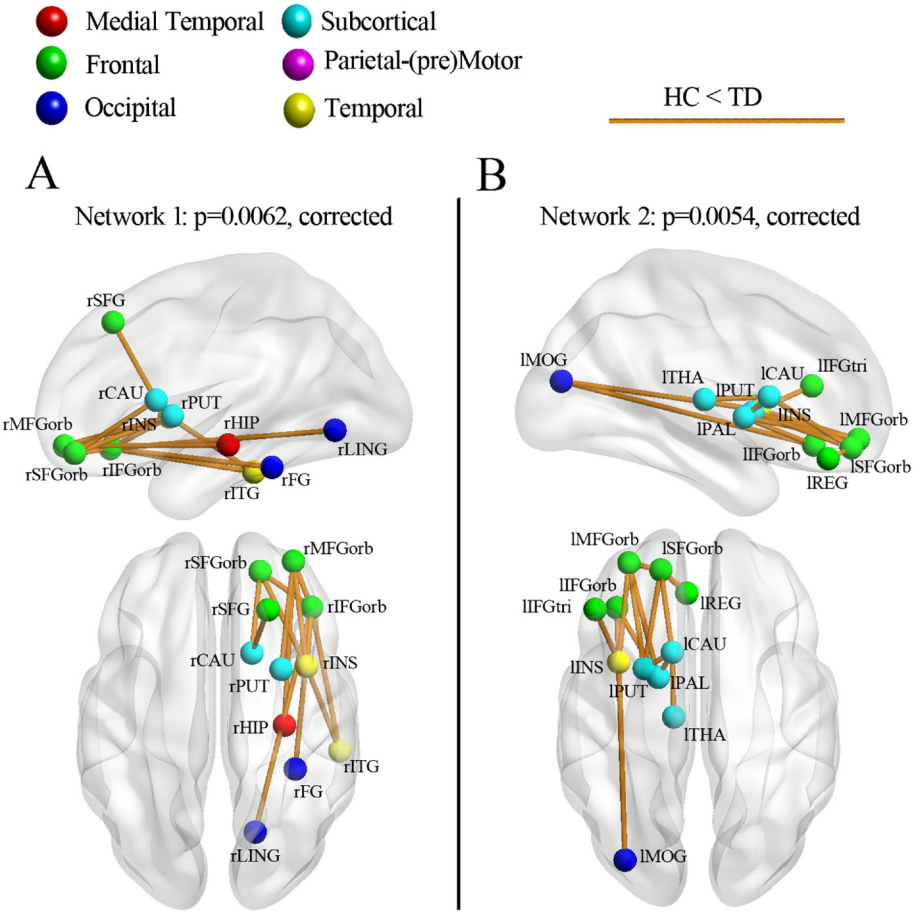

Fig. 3. Schematic of two altered sub-networks in TD patients mainly consisting of orbitofrontal structural connectivity within the right hemisphere (A) and the left hemisphere (B), revealed by NBS analysis. Labels indicate anatomical regions placed at their respective centroids. The six anatomical sub-regions listed in Table 2 are colored differently. The undirected edges indicate the increased connections in TD patients compared with HC. NBS, network based statistics; HC, healthy control; TD, treatment-naïve depression. (For interpretation of the references to color in this figure legend, the reader is referred to the web version of this article.)

large-scale SCN, which indicated that the nature of small-world architecture was conserved in the disease.

Despite the common small-world topology, significant differences in topological measures were observed between TD patients and HC. Although a recent study (Korgaonkar et al., in press) with a large sample of subjects reported no significant differences in topological measures of SCN between patients with depression and HC, their results might be affected by antidepressant effects. In contrast, aberrant topological organization of SCN observed in the present study was consistent with those reported in previous functional studies of depression. A study on functional connectivity network of TD patients reported significantly lower L and λ, and higher E_{global} relative to HC, indicating that TD patients showed increased long-distance functional connectivity (J. Zhang et al., 2011). Electroencephalogram studies reported that depression had significantly smaller λ and γ compared with HC, suggesting a loss of synchronization between distant neurons and low efficiency of local information processing (Leistedt et al., 2009; Sun et al., 2011). The altered topological organization of SCN found in our current study might provide evidence of structural substrates of the functional disturbance, indicating that an optimal balance between local specialization and global integration in TD patients was less effective than that in HC.

4.2. Altered orbitofrontal structural connectivity

The second major finding in our current study was the altered orbitofrontal structural connectivity of TD patients. The OFC is considered vital to a wide range of cognitive tasks, such as emotional face task (Townsend et al., 2010), decision-making and expectation (Kringelbach, 2005), working memory (Barbey et al., 2011), and coding of exteroceptive and interoceptive information (Price, 1999). In animals, OFC lesions resulted in lower thresholds for aggressive reactions, alterations in appetite, and increases in social withdrawal (Raleigh and Steklis, 1981). In human studies, evidence indicated that several mood disorders are associated with dysfunction of OFC. These disorders include patients with obsessive compulsive disorder (Chamberlain et al., 2008), bipolar disorder (Cotter et al., 2005) and social anxiety disorder (Liu et al., 2013). These studies suggested that OFC is associated with abnormalities in a wide range of affective behavior including depressed mood, anger, affective instability, fear, and anxiety symptoms, which were frequently observed in depressive patients. It may speculate that depression has OFC dysfunction.

Indeed, neurobiological evidence has supported clinical and neurobehavioral theoretical models regarding the involvement of the OFC in the pathophysiology of depression. In a postmortem study, Rajkowska et al. (1999) found significant cortical thinning of the OFC in depressive patients compared with HC. Using magnetic resonance imaging, Lai et al. (2000) and Bremner et al. (2002) reported bilateral reductions of OFC volumes in depression. Functional connectivity bias of the OFC was also investigated in drug-free depressive patients using fMRI face-matching task (Frodl et al., 2010). The potential importance of OFC in the pathophysiology of depression was also suggested by a cytoarchitectural study (Rajkowska et al., 2005), which found a reduction in the pyramidal neuron density of OFC in elderly depression.

Table 3
Altered connected sub-networks in TD patients compared with HC.

Region 1	Classification	Region 2	Classification	Mean w(e)		df	t value
				HC	TD		
Increased connections in network 1, p = 0.0062, corrected							
rSFGorb	Frontal	rIFGorb	Frontal	0.013	0.056	39	−3.70
rMFGorb	Frontal	rIFGorb	Frontal	0.027	0.084	39	−2.86
rSFGorb	Frontal	rINS	Temporal	0.011	0.028	39	−4.14
rMFGorb	Frontal	rINS	Temporal	0.010	0.035	39	−4.14
rIFGorb	Frontal	rINS	Temporal	0.023	0.063	39	−4.04
rMFGorb	Frontal	rHIP	Subcortical	0.003	0.022	39	−3.25
rIFGorb	Frontal	rLING	Occipital	0.002	0.014	39	−3.45
rIFGorb	Frontal	rFG	Occipital	0.004	0.018	39	−3.04
rSFG	Frontal	rCAU	Subcortical	0.004	0.014	39	−2.80
rSFGorb	Frontal	rCAU	Subcortical	0.003	0.017	39	−3.65
rMFGorb	Frontal	rPUT	Subcortical	0.006	0.028	39	−2.99
rIFGorb	Frontal	rITG	Temporal	0.003	0.016	39	−2.86
rINS	Temporal	rITG	Temporal	0.004	0.012	39	−2.61
Increased connections in network 2, p = 0.0054, corrected							
lSFGorb	Frontal	lMFGorb	Frontal	0.093	0.173	39	−2.54
lSFGorb	Frontal	lREG	Frontal	0.047	0.097	39	−2.58
lMFGorb	Frontal	lINS	Temporal	0.031	0.058	39	−2.60
lIFGtri	Frontal	lINS	Temporal	0.023	0.044	39	−2.53
lIFGorb	Frontal	lMOG	Occipital	0.002	0.011	39	−3.16
lINS	Temporal	lMOG	Occipital	0.005	0.015	39	−3.21
lSFGorb	Frontal	lCAU	Subcortical	0.002	0.010	39	−3.53
lSFGorb	Frontal	lPUT	Subcortical	0.005	0.017	39	−2.78
lMFGorb	Frontal	lPUT	Subcortical	0.010	0.038	39	−3.70
lCAU	Subcortical	lPUT	Subcortical	0.010	0.020	39	−3.43
lMFGorb	Frontal	lPAL	Subcortical	0.015	0.068	39	−3.86
lIFGorb	Frontal	lPAL	Subcortical	0.007	0.032	39	−2.90
lCAU	Subcortical	lPAL	Subcortical	0.009	0.021	39	−2.89
lCAU	Subcortical	lTHA	Subcortical	0.011	0.032	39	−3.72

Network-based statistics revealed two altered connected sub-networks in patients with TD, consisting of orbitofrontal connections with subcortical regions, and several temporal, occipital brain regions. The abbreviations of brain areas are listed in Table 2. TD, treatment-naive depression; HC, healthy control; df, degrees of freedom.

These morphological abnormalities and neuron reduction of OFC may imply the disruption of the structural connectivity of this region in depression. The altered orbitofrontal structural connectivity in TD patients observed in the present study may support this hypothesis.

The increased structural connectivity of the OFC with subcortical regions in the present study might be involved with the abnormal stimulus-reward association observed in depression. Several studies supported this hypothesis. For instance, studies on rats and monkeys found that lesions of the ventral striatum and pallidum, the mediodorsal thalamic nucleus, or the orbital medial prefrontal cortex caused deficits in stimulus-reward reversal tasks, in which the animals had difficulty switching from previously rewarded to unrewarded stimuli (Ferry et al., 2000; Kazama and Bachevalier, 2009; McBride and Slotnick, 1997; Roberts et al., 1990). In human studies, Forbes et al. (2006) found that young people with depression exhibited less neural response than HC in reward-related regions, including the caudate and OFC during the reward anticipation and outcome phases of reward processing.

The altered structural connectivity of the OFC with hippocampus in TD might be associated with biased memory for negative stimuli. For instance, an fMRI study (Hamilton and Gotlib, 2008) reported a greater functional connectivity of the hippocampus with the amygdala in depressive participants than in non-depressive participants during the encoding of remembered negative stimuli. The altered connectivity of the OFC with insula cortex might be involved in the emotion processing bias in TD patients (Disner et al., 2011). For example, Surguladze et al. (2010) found greater activation of the left insula in facial expressions of disgust in depression, which suggested hyperreactivity to disgust in depression. The disrupted connectivity of the OFC with several occipital regions might indicate biased attention for emotional stimuli, which suggested that TD patients had selective attention toward sad stimuli (Disner et al., 2011; Surguladze et al., 2005).

In summary, our results were consistent with a previously proposed neurobiological model of depression (Price and Drevets, 2012). Specifically, a loss of top-down regulation, that is, the suppression of prefrontal activity on limbic brain areas, is thought to be involved in the pathogenesis of emotional, behavioral, and cognitive changes in depression (Savitz and Drevets, 2009). For example, aberrant functional connectivity between cortico-limbic brain regions was observed in depression when they performed emotion processing tasks (Frodl et al., 2010; Kong et al., 2013). Additionally, the altered structural connectivity of OFC in the present study was found at the early stage of adult onset, probably highlighting importance of early diagnose and treatment of depression.

4.3. Limitations

Several limitations in the present study need to be mentioned. First, information about co-morbidity rate in TD patients and family income across two groups were not included, which might have led to confounded results (Kaufman and Charney, 2001; Lipina and Posner, 2012). Hence, future studies should include such information. Second, the present study might increase Type II error because of the small sample size. Thus, future researches should involve a larger sample size of depressive patients. Third, the findings of our current study might have been affected by fiber crossings during network construction using the FACT algorithm. Thus, succeeding research should use diffusion spectrum imaging techniques. Fourth, the parcellation scheme used to divide the whole brain into 90 sub-regions was based on the AAL template. However, several studies reported that different schemes could result in distinct topological patterns (Fornito et al., 2010; Sanabria-Diaz et al., 2010). Hence, further studies should combine multiple parcellation strategies to explore the effect on network topology in depression. Finally, the anatomical pathways constructed from DTI largely constrained the functional dynamics between distributed regions. Accordingly, a combined analysis of multi-modal imaging data would yield more information about interactions of brain structure and function in TD patients.

5. Conclusion

In conclusion, the present study aimed to investigate whole brain network organization and structural connectivity in TD patients using DTI tractography and graph theory. Altered structurally topological properties (decreased L, γ, λ, and σ, and increased E_{global} and E_{local}) suggested a functional disturbance between local specialization and global integration in TD patients. Disrupted orbitofrontal structural connectivity with hippocampus, insula, fusiform gyrus and several subcortical regions might indicate cognitive bias (e.g., biased memory, biased attention and biased emotion processing) in depression at early stage of adult onset. The results provided essential structural substrates for future research efforts to understand better the pathophysiology underlying depression.

Contributors

Dr. Chen H designed the study along with Dr. Zhao J. Drs. Liu F, Wang Y, and Zeng L collected the original imaging data. Drs. Long Z and Liu F managed and analyzed the imaging data. Drs. Long Z and Duan X wrote the first draft of the manuscript. All authors contributed to and have approved the final manuscript.

Conflicts of interest

The authors declare that they have no competing financial interests.

Acknowledgments

This work was supported by the 973 project 2012CB517901, the Natural Science Foundation of China (Grant Nos. 61125304, 61035006, 81171406, 30900483, 81301279 and 91132721), the Scholarship Award for Excellent Doctoral Student granted by the Ministry of Education (Grant No. A03003023901010), the special funding by the Ministry of Health of the Peoples' Republic of China (Grant No. 201002003), and the Fundamental Research Funds for the Central Universities (ZYGX2013Z004).

References

Achard S, Bullmore E. Efficiency and cost of economical brain functional networks. PLoS Comput Biol 2007;3:e17.
Anand A, Li Y, Wang Y, Lowe MJ, Dzemidzic M. Resting state corticolimbic connectivity abnormalities in unmedicated bipolar disorder and unipolar depression. Psychiatry Res Neuroimaging 2009;171:189–98.
Bai F, Shu N, Yuan Y, Shi Y, Yu H, Wu D, et al. Topologically convergent and divergent structural connectivity patterns between patients with remitted geriatric depression and amnestic mild cognitive impairment. J Neurosci 2012;32:4307–18.
Barbey AK, Koenigs M, Grafman J. Orbitofrontal contributions to human working memory. Cereb Cortex 2011;21:789–95.
Bremner JD, Vythilingam M, Vermetten E, Nazeer A, Adil J, Khan S, et al. Reduced volume of orbitofrontal cortex in major depression. Biol Psychiatry 2002;51:273–9.
Bullmore ET, Bassett DS. Brain graphs: graphical models of the human brain connectome. Annu Rev Clin Psychol 2011;7:113–40.
Chamberlain SR, Menzies L, Hampshire A, Suckling J, Fineberg NA, del Campo N, et al. Orbitofrontal dysfunction in patients with obsessive–compulsive disorder and their unaffected relatives. Science 2008;321:421–2.
Chantiluke K, Halari R, Simic M, Pariante CM, Papadopoulos A, Giampietro V, et al. Fronto-striato-cerebellar dysregulation in adolescents with depression during motivated attention. Biol Psychiatry 2012;71:59–67.
Cotter D, Hudson L, Landau S. Evidence for orbitofrontal pathology in bipolar disorder and major depression, but not in schizophrenia. Bipolar Disord 2005;7:358–69.
Disner SG, Beevers CG, Haigh EA, Beck AT. Neural mechanisms of the cognitive model of depression. Nat Rev Neurosci 2011;12:467–77.
Fang P, Zeng LL, Shen H, Wang L, Li B, Liu L, et al. Increased cortical-limbic anatomical network connectivity in major depression revealed by diffusion tensor imaging. PLoS One 2012;7:e45972.
Ferry AT, Lu XC, Price JL. Effects of excitotoxic lesions in the ventral striatopallidal–thalamocortical pathway on odor reversal learning: inability to extinguish an incorrect response. Exp Brain Res 2000;131:320–35.
Forbes EE, Christopher May J, Siegle GJ, Ladouceur CD, Ryan ND, Carter CS, et al. Reward-related decision-making in pediatric major depressive disorder: an fMRI study. J Child Psychol Psychiatry 2006;47:1031–40.
Fornito A, Zalesky A, Bullmore ET. Network scaling effects in graph analytic studies of human resting-state FMRI data. Front Syst Neurosci 2010;4:22.
Frodl T, Bokde AL, Scheuerecker J, Lisiecka D, Schoepf V, Hampel H, et al. Functional connectivity bias of the orbitofrontal cortex in drug-free patients with major depression. Biol Psychiatry 2010;67:161–7.
Gong G, He Y, Concha L, Lebel C, Gross DW, Evans AC, et al. Mapping anatomical connectivity patterns of human cerebral cortex using in vivo diffusion tensor imaging tractography. Cereb Cortex 2009;19:524–36.
Guo W, Liu F, Dai Y, Jiang M, Zhang J, Yu L, et al. Decreased interhemispheric resting-state functional connectivity in first-episode, drug-naive major depressive disorder. Prog Neuro-Psychopharmacol Biol Psychiatry 2013a;41:24–9.
Guo W, Liu F, Xue Z, Gao K, Liu Z, Xiao C, et al. Abnormal resting-state cerebellar–cerebral functional connectivity in treatment-resistant depression and treatment sensitive depression. Prog Neuro-Psychopharmacol Biol Psychiatry 2013b;44:51–7.
Hagmann P, Cammoun L, Gigandet X, Meuli R, Honey CJ, Wedeen VJ, et al. Mapping the structural core of human cerebral cortex. PLoS Biol 2008;6:e159.
Hamilton M. Development of a rating scale for primary depressive illness. Br J Soc Clin Psychol 1967;6:278–96.
Hamilton JP, Gotlib IH. Neural substrates of increased memory sensitivity for negative stimuli in major depression. Biol Psychiatry 2008;63:1155–62.
He Y, Evans A. Graph theoretical modeling of brain connectivity. Curr Opin Neurol 2010;23:341–50.
Honey CJ, Sporns O, Cammoun L, Gigandet X, Thiran JP, Meuli R, et al. Predicting human resting-state functional connectivity from structural connectivity. Proc Natl Acad Sci U S A 2009;106:2035–40.
Hooley JM, Gruber SA, Parker HA, Guillaumot J, Rogowska J, Yurgelun-Todd DA. Cortico-limbic response to personally challenging emotional stimuli after complete recovery from depression. Psychiatry Res 2009;172:83–91.
Jia Z, Huang X, Wu Q, Zhang T, Lui S, Zhang J, et al. High-field magnetic resonance imaging of suicidality in patients with major depressive disorder. Am J Psychiatry 2010;167:1381–90.
Jin C, Gao C, Chen C, Ma S, Netra R, Wang Y, et al. A preliminary study of the dysregulation of the resting networks in first-episode medication-naive adolescent depression. Neurosci Lett 2011;503:105–9.
Kaufman J, Charney D. Effects of early stress on brain structure and function: implications for understanding the relationship between child maltreatment and depression. Dev Psychopathol 2001;13:451–71.
Kazama A, Bachevalier J. Selective aspiration or neurotoxic lesions of orbital frontal areas 11 and 13 spared monkeys' performance on the object discrimination reversal task. J Neurosci 2009;29:2794–804.
Kong LT, Chen KY, Tang YQ, Wu F, Driesen N, Womer F, et al. Functional connectivity between the amygdala and prefrontal cortex in medication-naive individuals with major depressive disorder. J Psychiatry Neurosci 2013;38:417–22.
Korgaonkar MS, Cooper NJ, Williams LM, Grieve SM. Mapping inter-regional connectivity of the entire cortex to characterize major depressive disorder: a whole-brain diffusion tensor imaging tractography study. Neuroreport 2012;23:566–71.
Korgaonkar MS, Fornito A, Williams LM, Grieve SM. Abnormal structural networks characterize major depressive disorder: a connectome analysis. Biol Psychiatry 2014. (in press).
Kringelbach ML. The human orbitofrontal cortex: linking reward to hedonic experience. Nat Rev Neurosci 2005;6:691–702.
Lai T, Payne ME, Byrum CE, Steffens DC, Krishnan KR. Reduction of orbital frontal cortex volume in geriatric depression. Biol Psychiatry 2000;48:971–5.
Latora V, Marchiori M. Efficient behavior of small-world networks. Phys Rev Lett 2001;87:198701.
Lee BT, Seok JH, Lee BC, Cho SW, Yoon BJ, Lee KU, et al. Neural correlates of affective processing in response to sad and angry facial stimuli in patients with major depressive disorder. Prog Neuro-Psychopharmacol Biol Psychiatry 2008;32:778–85.
Leistedt SJ, Coumans N, Dumont M, Lanquart JP, Stam CJ, Linkowski P. Altered sleep brain functional connectivity in acutely depressed patients. Hum Brain Mapp 2009;30:2207–19.
Li M, Chen H, Wang J, Liu F, Long Z, Wang Y, et al. Handedness- and hemisphere-related differences in small-world networks: a diffusion tensor imaging tractography study. Brain Connect 2014;4(2):145–56.
Lipina SJ, Posner MI. The impact of poverty on the development of brain networks. Front Hum Neurosci 2012;6:238.
Liu L, Zeng LL, Li Y, Ma Q, Li B, Shen H, et al. Altered cerebellar functional connectivity with intrinsic connectivity networks in adults with major depressive disorder. PLoS One 2012;7:e39516.
Liu F, Guo W, Fouche JP, Wang Y, Wang W, Ding J, et al. Multivariate classification of social anxiety disorder using whole brain functional connectivity. Brain Struct Funct 2013. http://dx.doi.org/10.1007/s00429-013-0641-4.
Lo CY, Wang PN, Chou KH, Wang J, He Y, Lin CP. Diffusion tensor tractography reveals abnormal topological organization in structural cortical networks in Alzheimer's disease. J Neurosci 2010;30:16876–85.
Long Z, Duan X, Xie B, Du H, Li R, Xu Q, et al. Altered brain structural connectivity in post-traumatic stress disorder: a diffusion tensor imaging tractography study. J Affect Disord 2013;150:798–806.
Lui S, Wu Q, Qiu L, Yang X, Kuang W, Chan RC, et al. Resting-state functional connectivity in treatment-resistant depression. Am J Psychiatry 2011;168:642–8.
Ma C, Ding J, Li J, Guo W, Long Z, Liu F, et al. Resting-state functional connectivity bias of middle temporal gyrus and caudate with altered gray matter volume in major depression. PLoS One 2012;7:e45263.
Marchand WR. Cortico-basal ganglia circuitry: a review of key research and implications for functional connectivity studies of mood and anxiety disorders. Brain Struct Funct 2010;215:73–96.
McBride SA, Slotnick B. The olfactory thalamocortical system and odor reversal learning examined using an asymmetrical lesion paradigm in rats. Behav Neurosci 1997;111:1273–84.
Onnela JP, Saramaki J, Kertesz J, Kaski K. Intensity and coherence of motifs in weighted complex networks. Phys Rev E Stat Nonlinear Soft Matter Phys 2005;71:065103.
Petersen T, Gordon JA, Kant A, Fava M, Rosenbaum JF, Nierenberg AA. Treatment resistant depression and axis I co-morbidity. Psychol Med 2001;31:1223–9.
Price JL. Prefrontal cortical networks related to visceral function and mood. Ann N Y Acad Sci 1999;877:383–96.
Price JL, Drevets WC. Neural circuits underlying the pathophysiology of mood disorders. Trends Cogn Sci 2012;16:61–71.
Rajkowska G, Miguel-Hidalgo JJ, Wei J, Dilley G, Pittman SD, Meltzer HY, et al. Morphometric evidence for neuronal and glial prefrontal cell pathology in major depression. Biol Psychiatry 1999;45:1085–98.
Rajkowska G, Miguel-Hidalgo JJ, Dubey P, Stockmeier CA, Krishnan KR. Prominent reduction in pyramidal neurons density in the orbitofrontal cortex of elderly depressed patients. Biol Psychiatry 2005;58:297–306.
Raleigh MJ, Steklis HD. Effect of orbitofrontal and temporal neocortical lesions of the affiliative behavior of vervet monkeys (*Cercopithecus aethiops sabaeus*). Exp Neurol 1981;73:378–89.
Roberts AC, Robbins TW, Everitt BJ, Jones GH, Sirkia TE, Wilkinson J, et al. The effects of excitotoxic lesions of the basal forebrain on the acquisition, retention and serial reversal of visual discriminations in marmosets. Neuroscience 1990;34:311–29.
Rubinov M, Sporns O. Complex network measures of brain connectivity: uses and interpretations. Neuroimage 2010;52:1059–69.
Runeson BS, Rich CL. Diagnostic and statistical manual of mental disorders, 3rd ed. (DSM-III), adaptive functioning in young Swedish suicides. Ann Clin Psychiatry 1994;6:181–3.
Sanabria-Diaz G, Melie-Garcia L, Iturria-Medina Y, Aleman-Gomez Y, Hernandez-Gonzalez G, Valdes-Urrutia L, et al. Surface area and cortical thickness descriptors reveal different attributes of the structural human brain networks. Neuroimage 2010;50:1497–510.

Savitz J, Drevets WC. Bipolar and major depressive disorder: neuroimaging the developmental–degenerative divide. Neurosci Biobehav Rev 2009;33:699–771.
Shu N, Liu Y, Li K, Duan Y, Wang J, Yu C, et al. Diffusion tensor tractography reveals disrupted topological efficiency in white matter structural networks in multiple sclerosis. Cereb Cortex 2011;21:2565–77.
Sporns O, Zwi JD. The small world of the cerebral cortex. Neuroinformatics 2004;2:145–62.
Sun Y, Hu S, Chambers J, Zhu Y, Tong S. Graphic patterns of cortical functional connectivity of depressed patients on the basis of EEG measurements. Conference proceedings: Annual International Conference of the IEEE Engineering in Medicine and Biology Society IEEE Engineering in Medicine and Biology Society Conference; 2011. p. 1419–22.
Surguladze S, Brammer MJ, Keedwell P, Giampietro V, Young AW, Travis MJ, et al. A differential pattern of neural response toward sad versus happy facial expressions in major depressive disorder. Biol Psychiatry 2005;57:201–9.
Surguladze SA, El-Hage W, Dalgleish T, Radua J, Gohier B, Phillips ML. Depression is associated with increased sensitivity to signals of disgust: a functional magnetic resonance imaging study. J Psychiatr Res 2010;44:894–902.
Townsend JD, Eberhart NK, Bookheimer SY, Eisenberger NI, Foland-Ross LC, Cook IA, et al. fMRI activation in the amygdala and the orbitofrontal cortex in unmedicated subjects with major depressive disorder. Psychiatry Res 2010;183:209–17.
Tzourio-Mazoyer N, Landeau B, Papathanassiou D, Crivello F, Etard O, Delcroix N, et al. Automated anatomical labeling of activations in SPM using a macroscopic anatomical parcellation of the MNI MRI single-subject brain. Neuroimage 2002;15:273–89.
van den Heuvel MP, Sporns O. Rich-club organization of the human connectome. J Neurosci 2011;31:15775–86.
van den Heuvel M, Mandl R, Luigjes J, Hulshoff Pol H. Microstructural organization of the cingulum tract and the level of default mode functional connectivity. J Neurosci 2008;28:10844–51.
Wang R, Beener T, Sorensen AVW. Diffusion toolkit: a software package for diffusion imaging data processing and tractography. Proc Int Soc Mag Reson Med 2007;3720.
Wang J, Zuo X, He Y. Graph-based network analysis of resting-state functional MRI. Front Syst Neurosci 2010;4:16.
Watts DJ, Strogatz SH. Collective dynamics of 'small-world' networks. Nature 1998;393:440–2.
Yue YY, Yuan YG, Hou ZH, Jiang WH, Bai F, Zhang ZJ. Abnormal functional connectivity of amygdala in late-onset depression was associated with cognitive deficits. PLoS One 2013;8.
Zalesky A, Fornito A, Bullmore ET. Network-based statistic: identifying differences in brain networks. Neuroimage 2010;53:1197–207.
Zhang J, Wang J, Wu Q, Kuang W, Huang X, He Y, et al. Disrupted brain connectivity networks in drug-naive, first-episode major depressive disorder. Biol Psychiatry 2011a;70:334–42.
Zhang Z, Liao W, Chen H, Mantini D, Ding JR, Xu Q, et al. Altered functional–structural coupling of large-scale brain networks in idiopathic generalized epilepsy. Brain 2011b;134:2912–28.
Zhu X, Wang X, Xiao J, Liao J, Zhong M, Wang W, et al. Evidence of a dissociation pattern in resting-state default mode network connectivity in first-episode, treatment-naive major depression patients. Biol Psychiatry 2012;71:611–7.